@RockMechLab_UoP

Fluid-driven fracture and seismicity in the shallow crust: Philip Benson, Stephan Gehne, Nathaniel Forbes Inskip, Philip Meredith & Nick Koor

Fluid-driven fracture: controversial and poorly understood

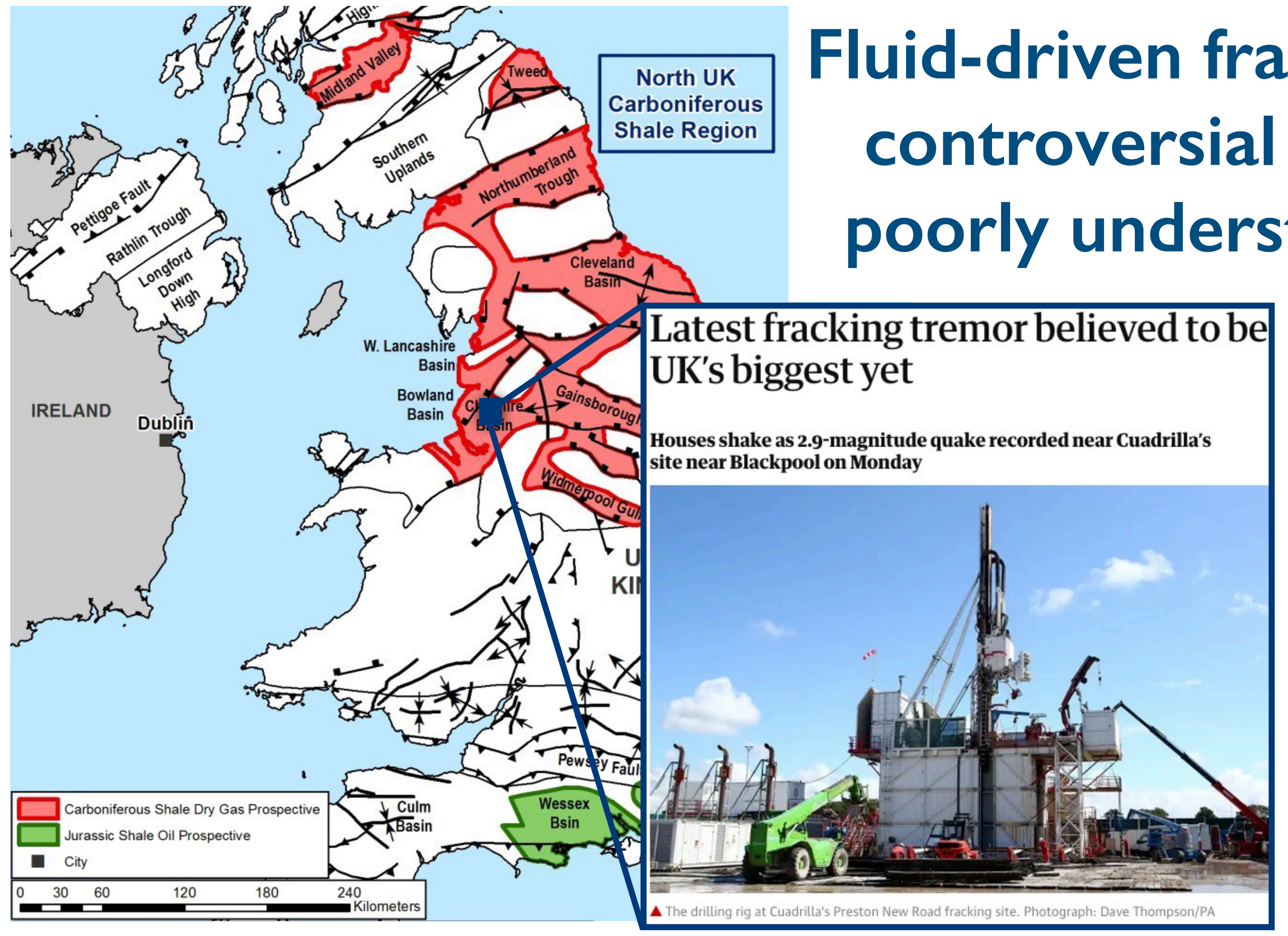

Nash Point shale

- Nash Point Shale was used, rather than the highly friable Bowland Shale
- Although not truly 'representative' of the rock at depth, the aims of this project seek to under stand the tensile fracture mechanics, and what seismicity this generated during these very dynamic processes
- Hence choice of rock type is less important than a laboratory protocol for measuring high speed fracture in simulated conditions.
- That said, the shale exhibits all the typical features expected of a mudstone, location (below) and properties (next pane):

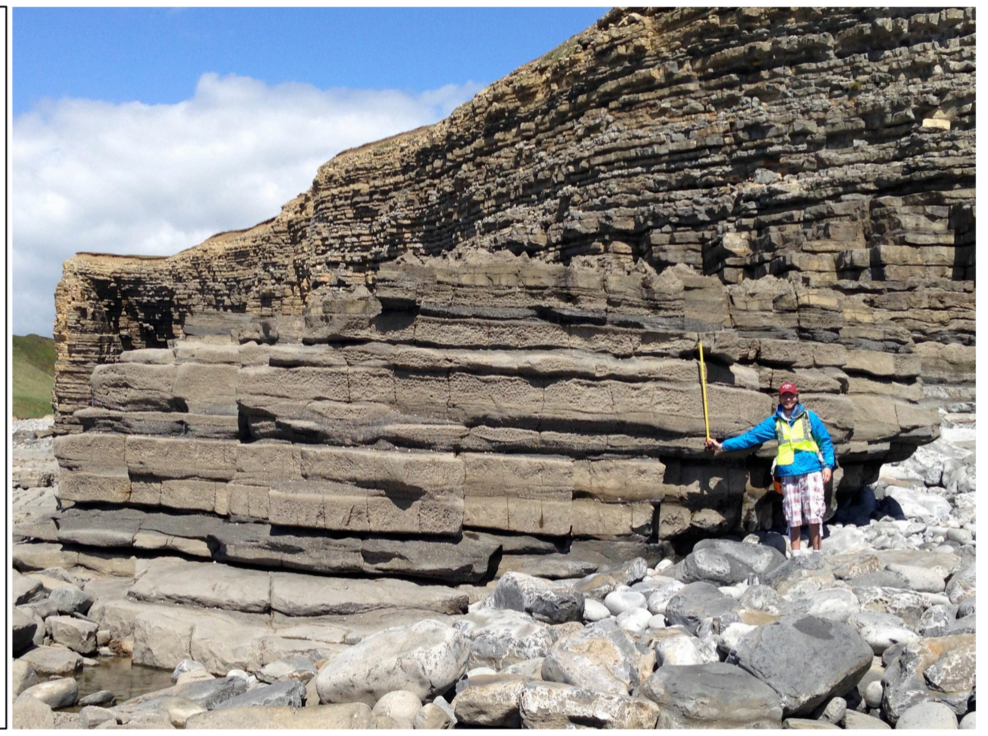

Gehne, PhD thesis, 2018
Forbes Inskip et al., JGR 2018

Porthkerry Member

(Blue Lias Formation)

- Early Jurassic age

(190-200 ma)

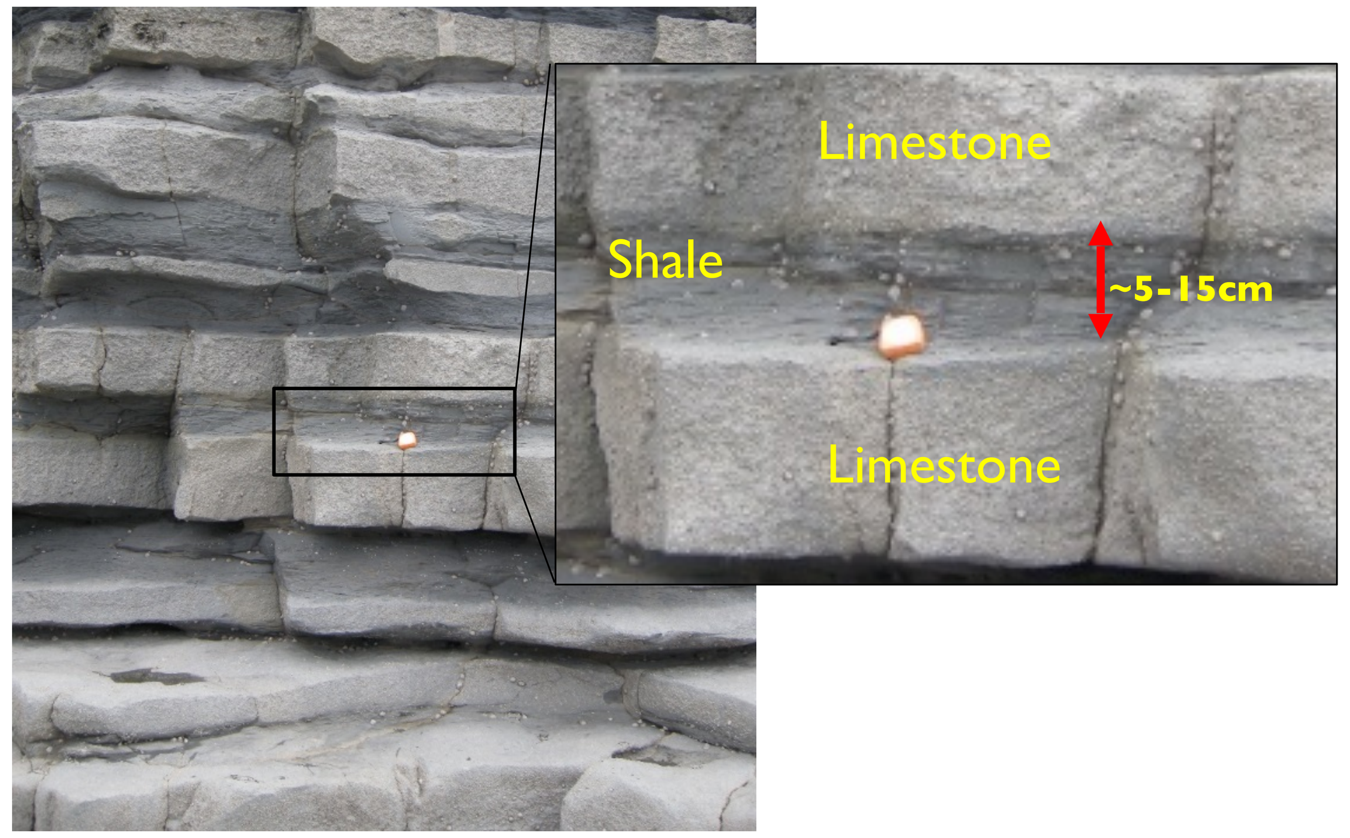

Nash Point Shale (NPS): physical properties

At ambient conditions:

- Highly anisotropic: Mechanical ~ 60%, (From indirect Brazilian disk tests)
- P-wave velocity anisotropy 56% (using data along and cross bedding)

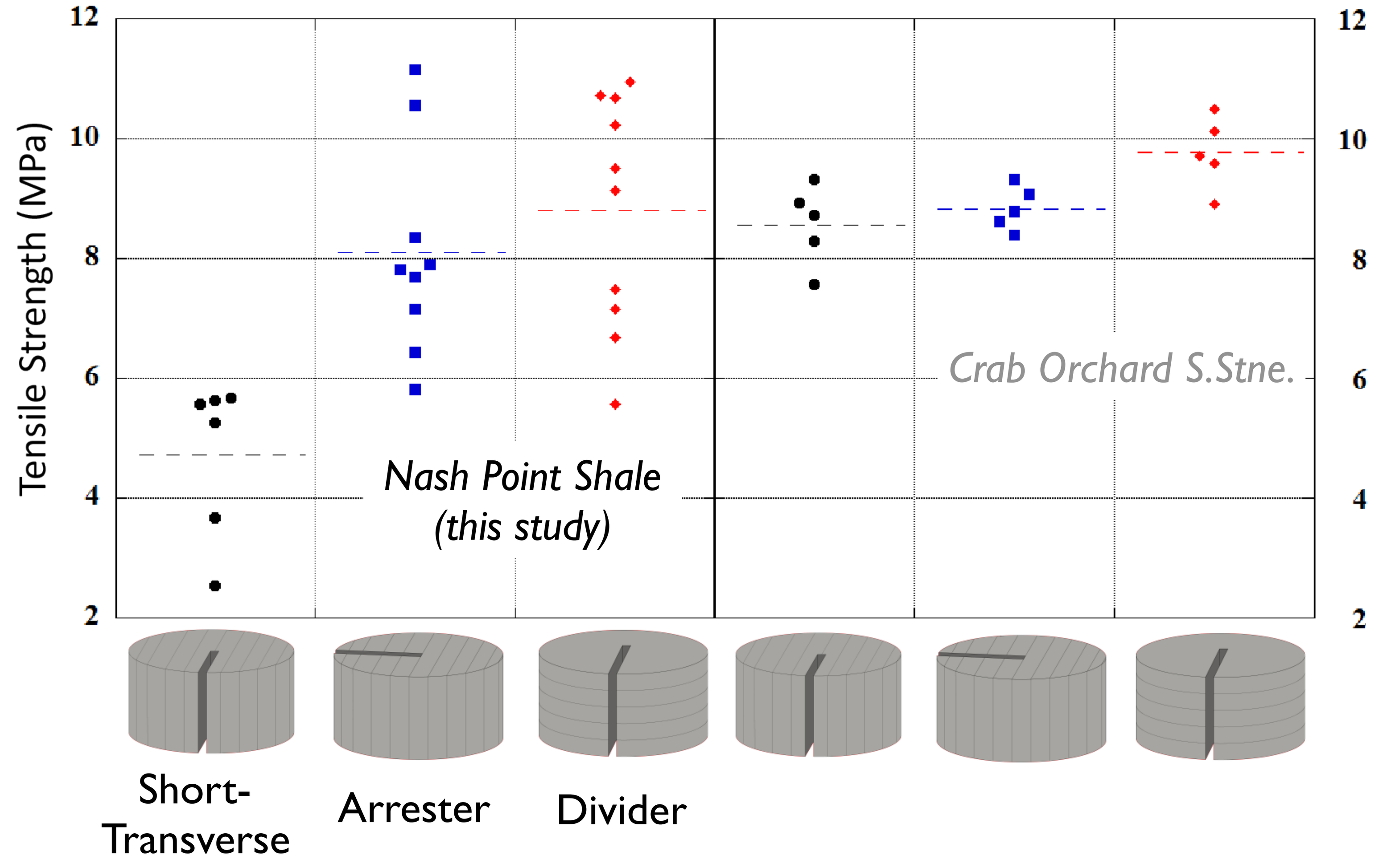

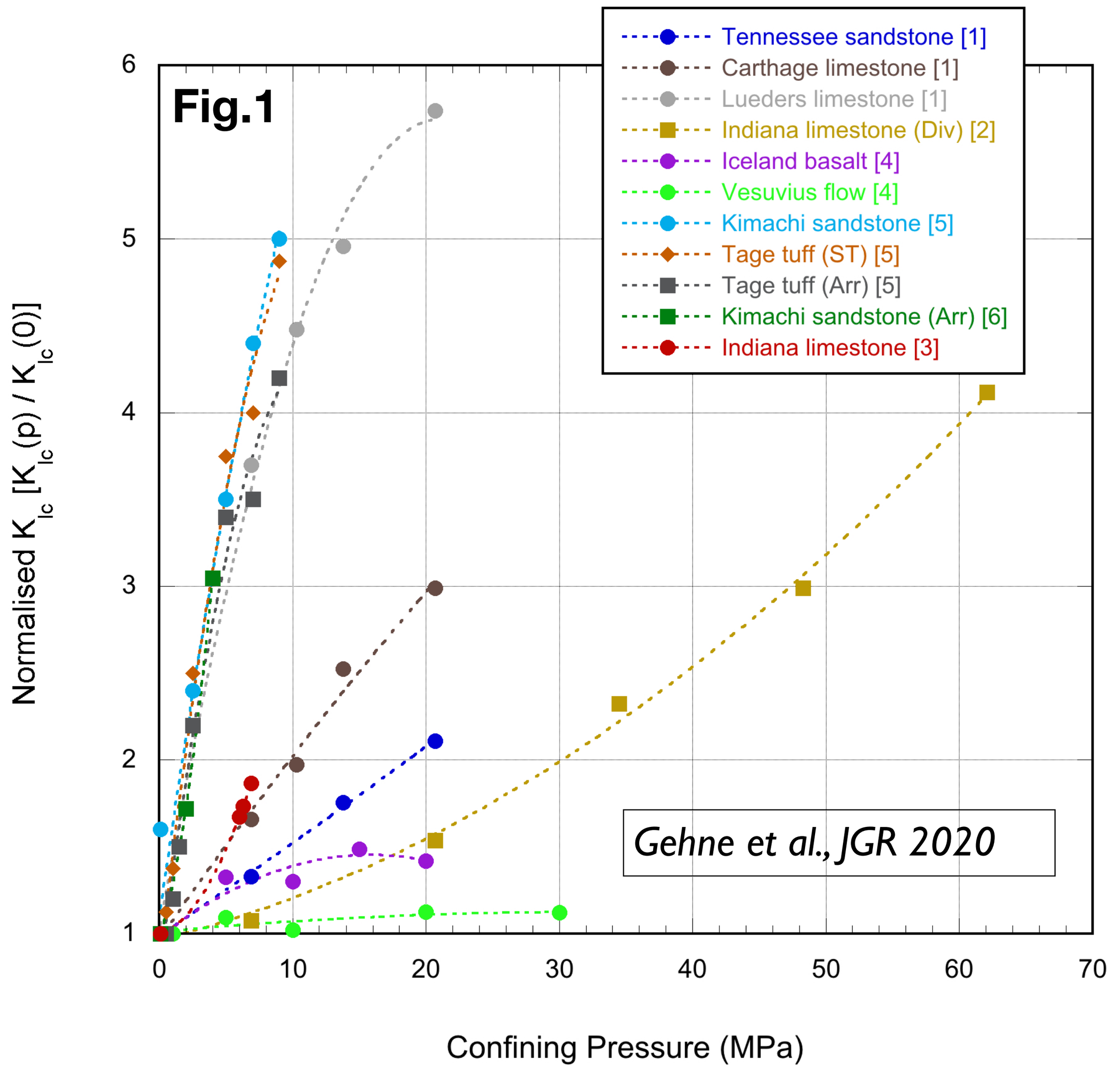

- During the project (designed to investigate fluid-driven fracture and coupled AE) a *secondary goal* was developed:
- Measuring fracture toughness (K_{Ic}) is a common parameter to understand stresses needed to extent a fracture
- This parameter is almost *never* measured at high confining pressure (left)

Fluid-driven fracture and seismicity in the shallow crust: Philip Benson, Stephan Gehne, Nathaniel Forbes Inskip, Philip Meredith & Nick Koor

Lab simulation of Fracking

Development: Stephan Gehne

Aims: Investigate tensile fracture via fluid overpressure; links to seismicity and anisotropy via *high-speed* data acquisition.

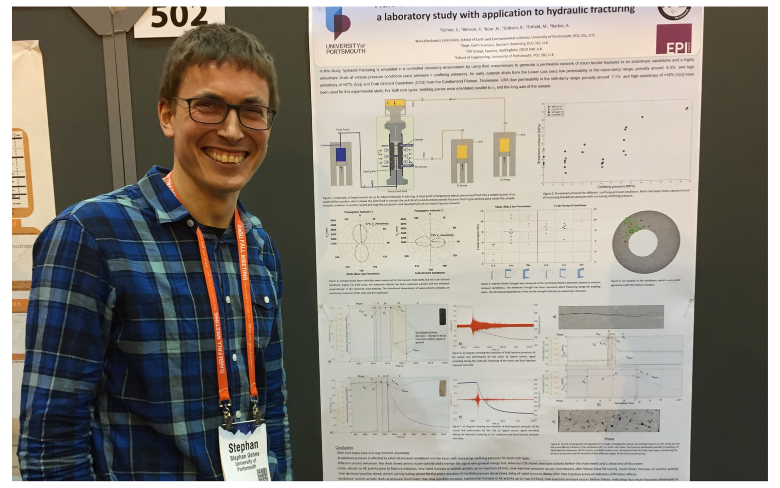

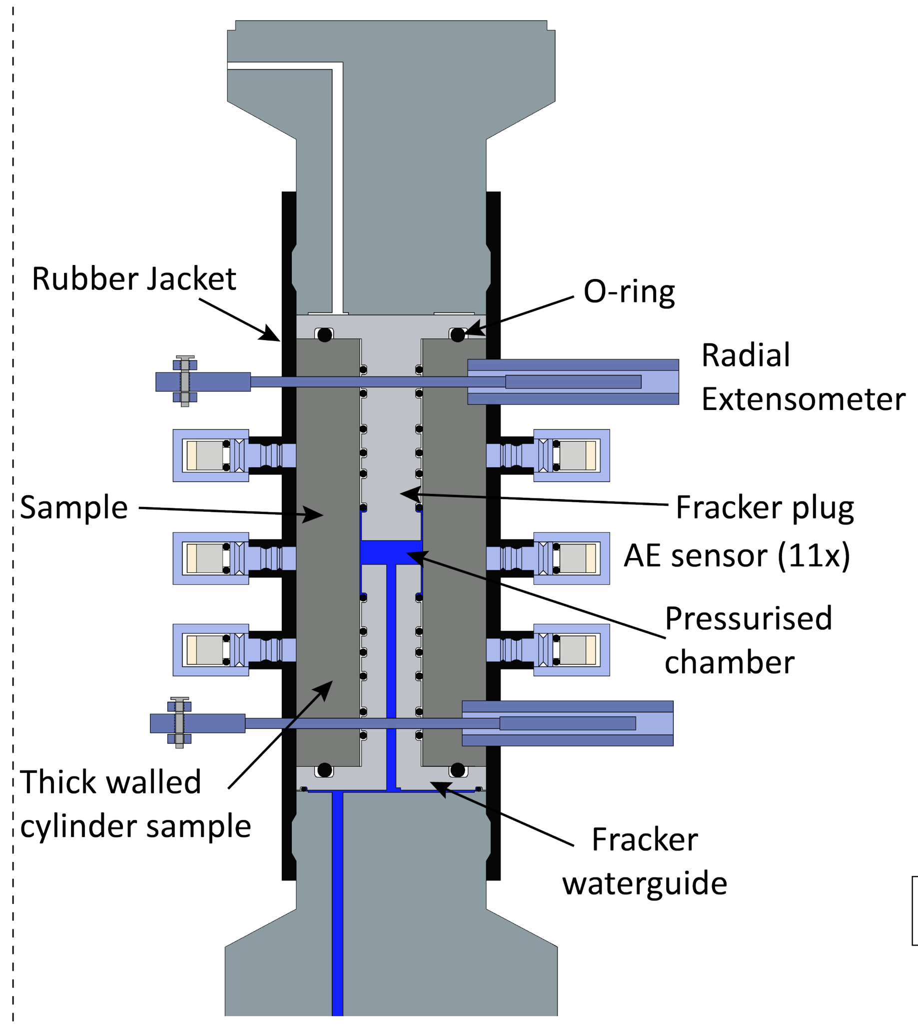

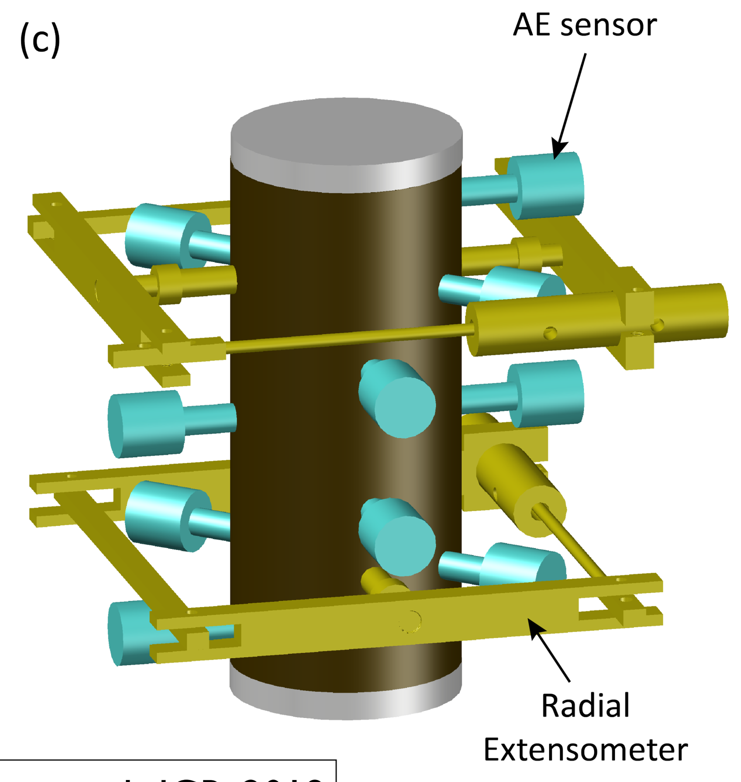

Gehne et al., JGR, 2019

- The sample setup above is housed in a standard conventional triaxial cell, with a small force applied to the top piston to ensure sealing at the top O-ring. This stress was never higher than 25% of the UCS value of the rock tested.
- 11 channels of AE are fed into a 'continuous' AE recorder which digitizes the AE sensor voltages (pre-amplified by 60 dB) at 10 MHz sampling rate (at 16 bit resolution) directly to hard-disk for later offline processing.
- A 12th channel records the Internal fluid pressure (also at 10MHz) in order to resolve the high speed fluid/fracture interaction during the hydraulic fracture event.
- The move method also allows the AE and pore fluid data to be perfectly synchronized.
- A second recording system digitizes and records the rest of the mechanical data (stress, strain, confining pressure, radial strain) at 10 kHz using a National Instruments DAQ board. Data synchronization between the two systems is achieved by using the common Internal fluid pressure sensor.

Hydraulic Fracture using a conventional triaxial apparatus: method

- A typical experiment is shown below, which takes approximately 500s.
- At a fixed test confining pressure (20MPa) here, fluid pressure is increased using a constant fluid volume injection rate of 1mL/minute. This pressurizes the closed system; the axial stress is set (via and electronic servo control loop) to track the fluid pressure with an additional 10 MPa to ensure sealing.
- The hydraulic fracture event lasts less than a second, signified by the drop in fluid pressure, accompanied by a ramped rise in radial deformation (green line).

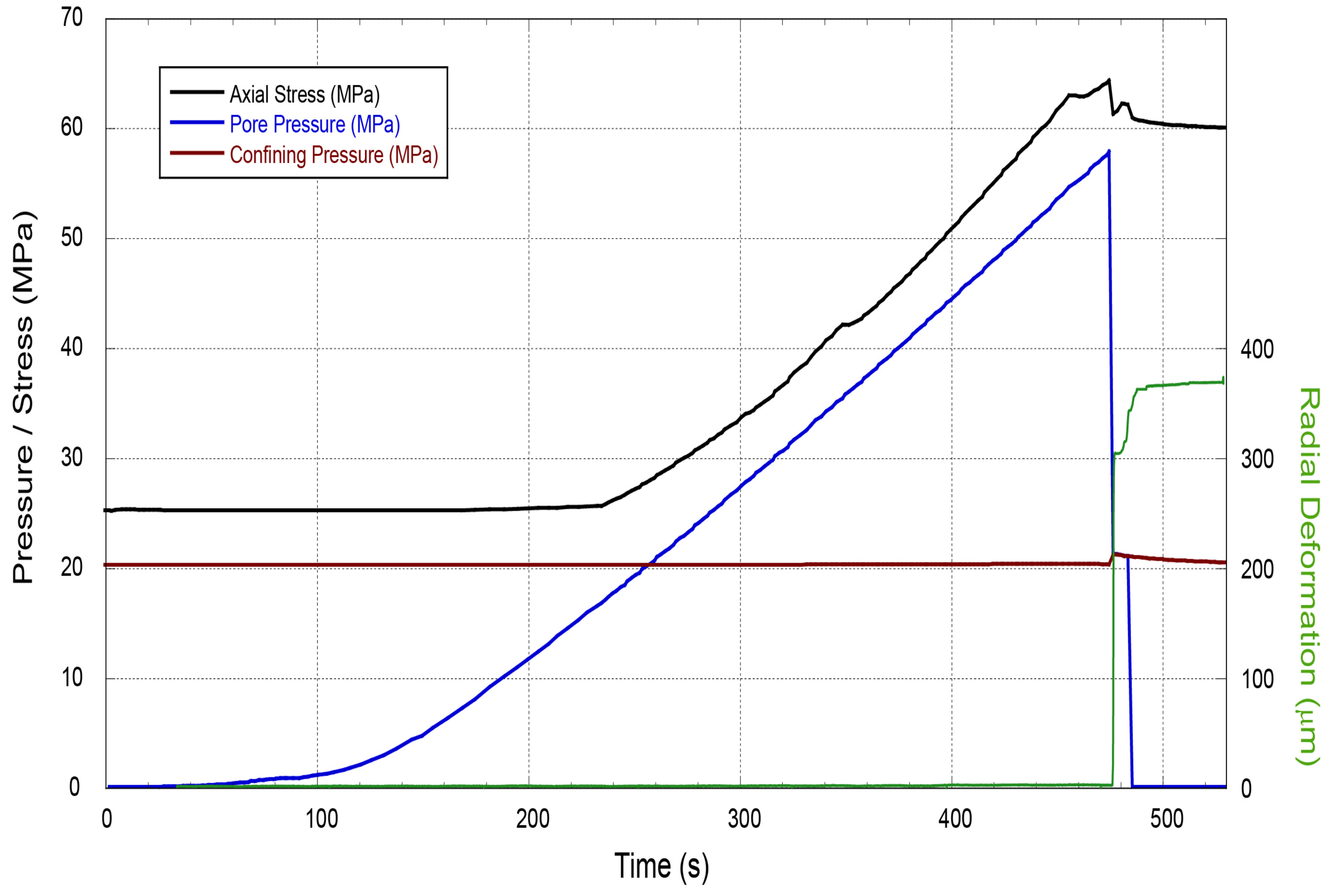

- Approximately 60 experiments were conducted between 2014-2018 using **N**ash **P**oint **S**hale and a smaller number with **C**rab **O**rchard **S**andstone:

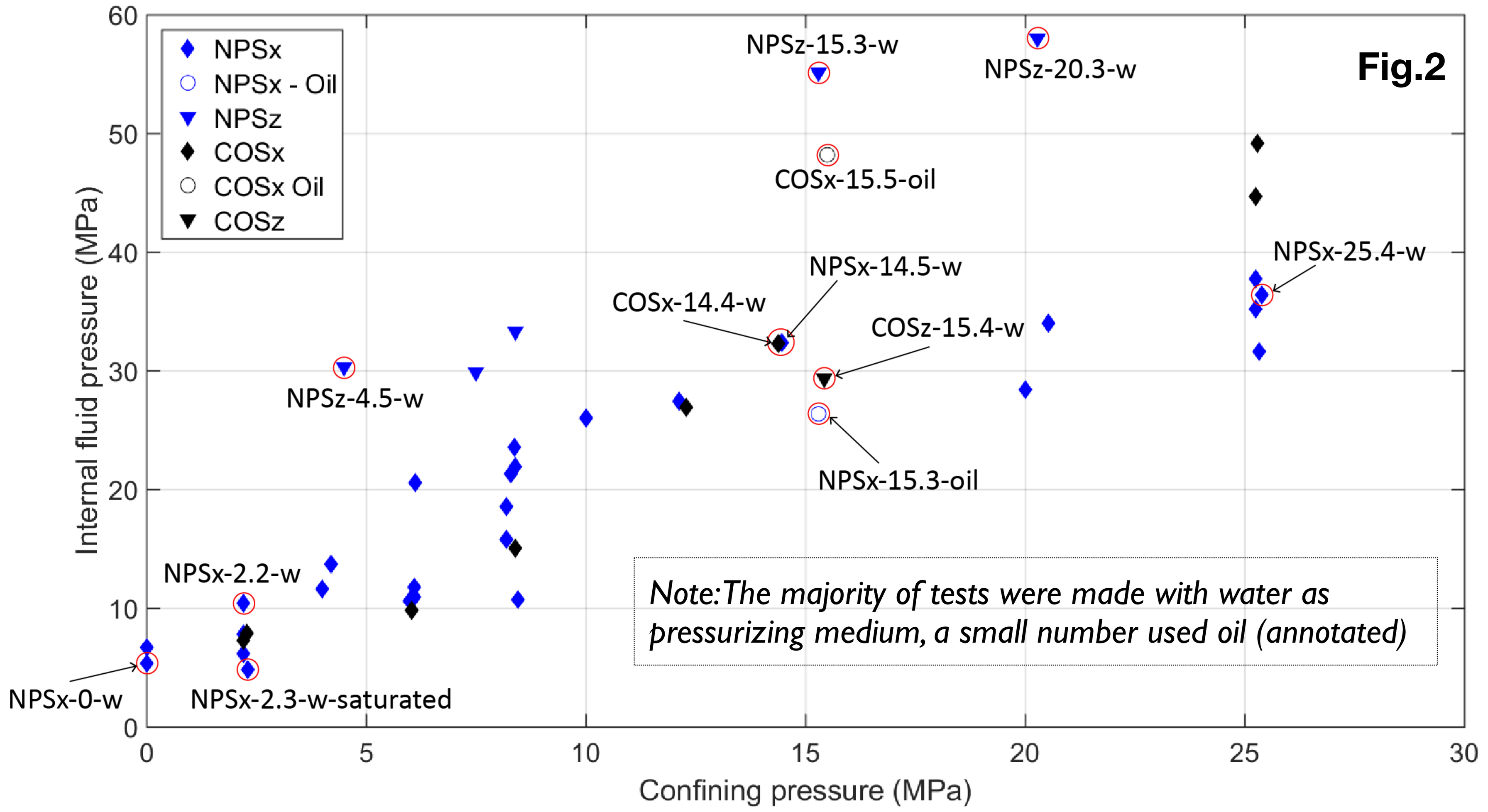

Typical microstructure results: (short-transverse mode)

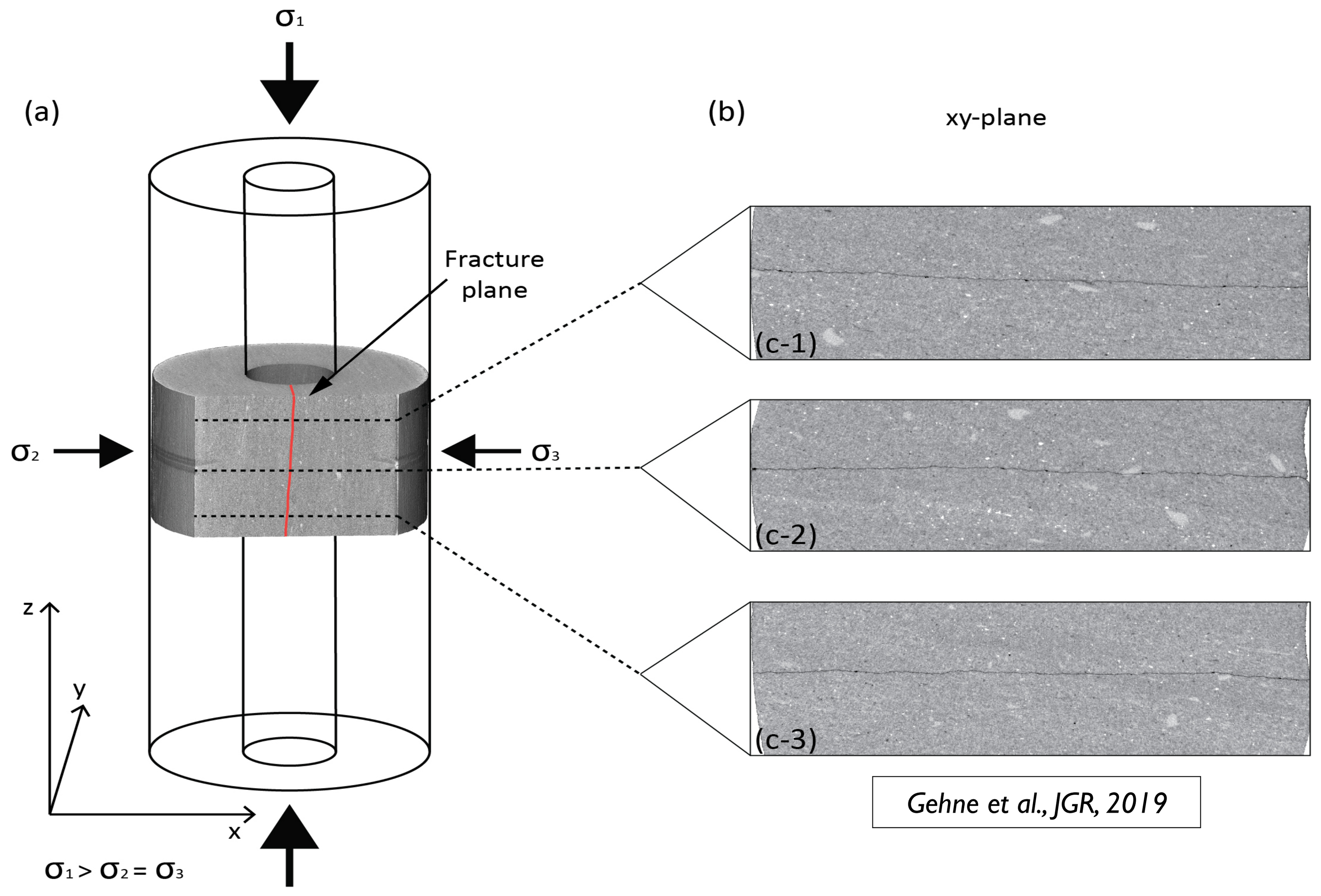

[Note: Arrester mode is not energetically favourable]

Typical microstructure results: (divider mode)

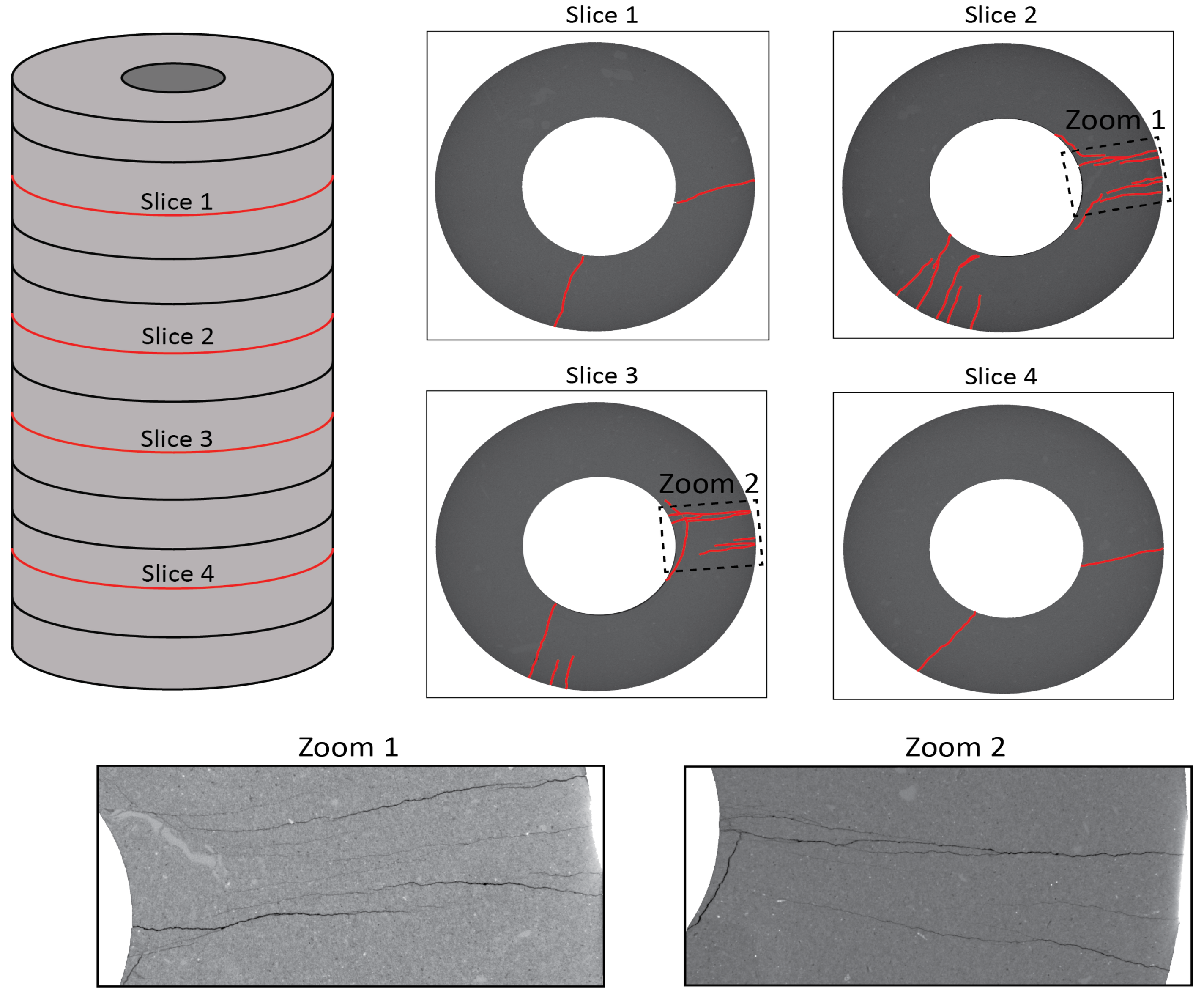

Fluid-driven fracture and seismicity in the shallow crust: Philip Benson, Stephan Gehne, Nathaniel Forbes Inskip, Philip Meredith & Nick Koor

Typical fluid-pressure / AE results: (short-transverse mode)

At ~**100m** simulated depth we note:

- Seismicity occurs before main fracture, but after maxPp
- Fluid pressure oscillations revealed
- Fluid oscillations mirror pressure
- Complex!

BUT: there is far more complexity to the results than the basic maximum Pp (breakdown pressure)

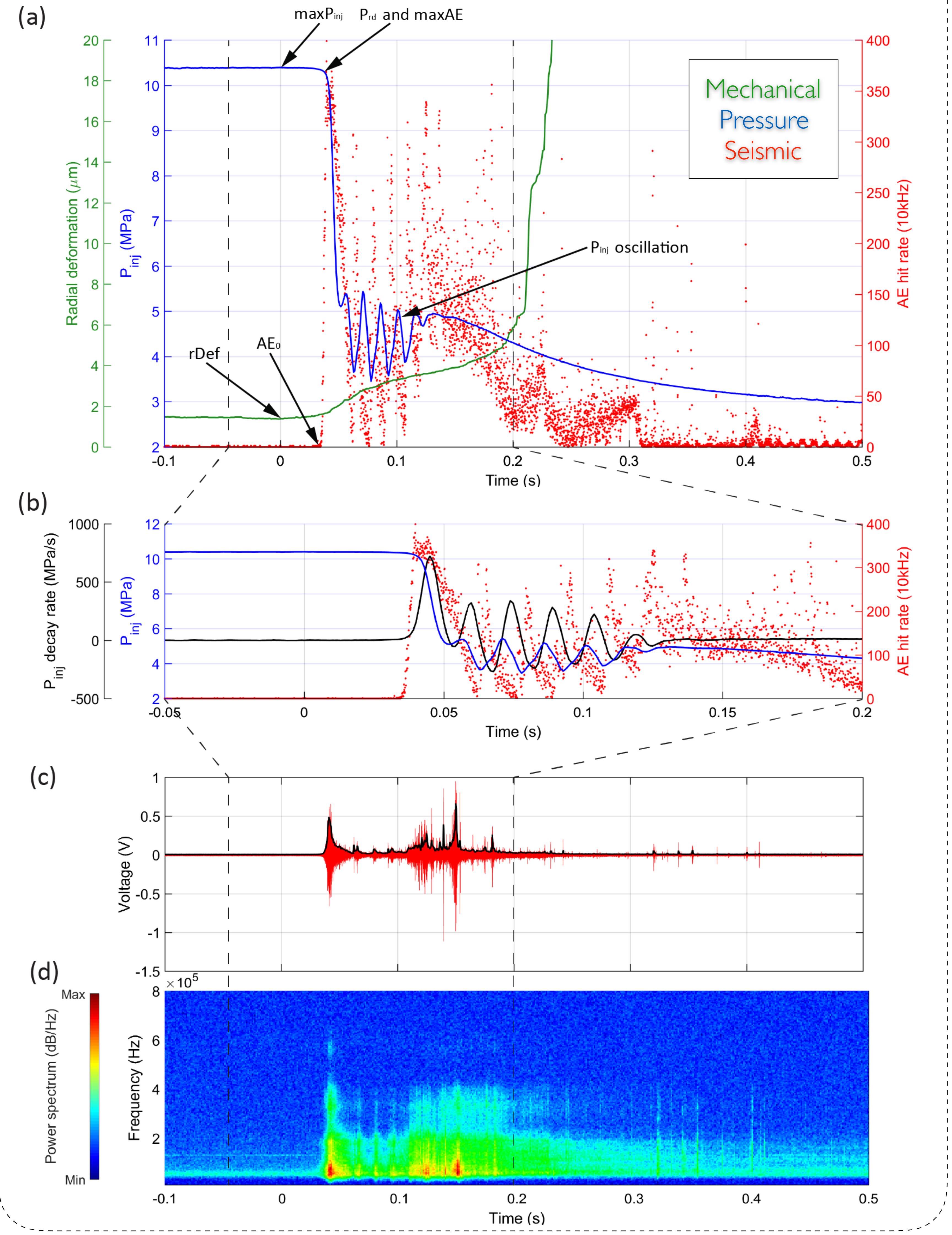

Typical fluid-pressure / AE results: (short-transverse mode)

At ~**800m** simulated depth we note:

- Seismicity again occurs before main fracture; shorter gap between AE and maxPp
- Fewer fluid pressure oscillations

BUT: there is far more complexity to the results than the basic maximum Pp (breakdown pressure)

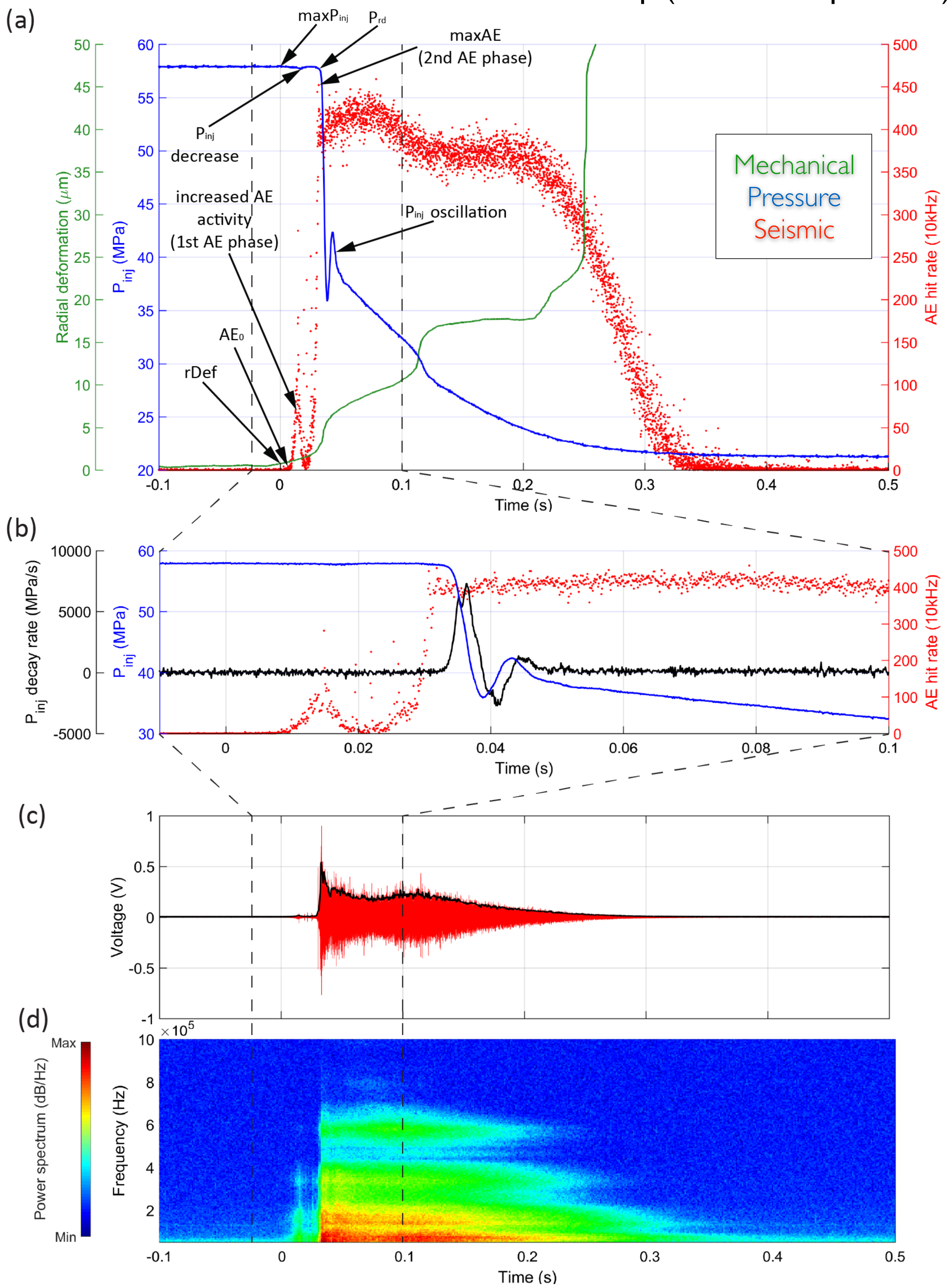

Q: what's the physical mechanism?

Where do those fluid pressure oscillations come from?

Working hypothesis:

- Each time pressure exceeds fracture toughness (K_{Ic}), fracture extends…
- This is accompanied by a burst in AE / energy…
- However the fluid is sill being injected so the pressure is re-established and the process repeats…
- Sequence finishes when fracture reaches the sample edge, fluid pressure decreases.

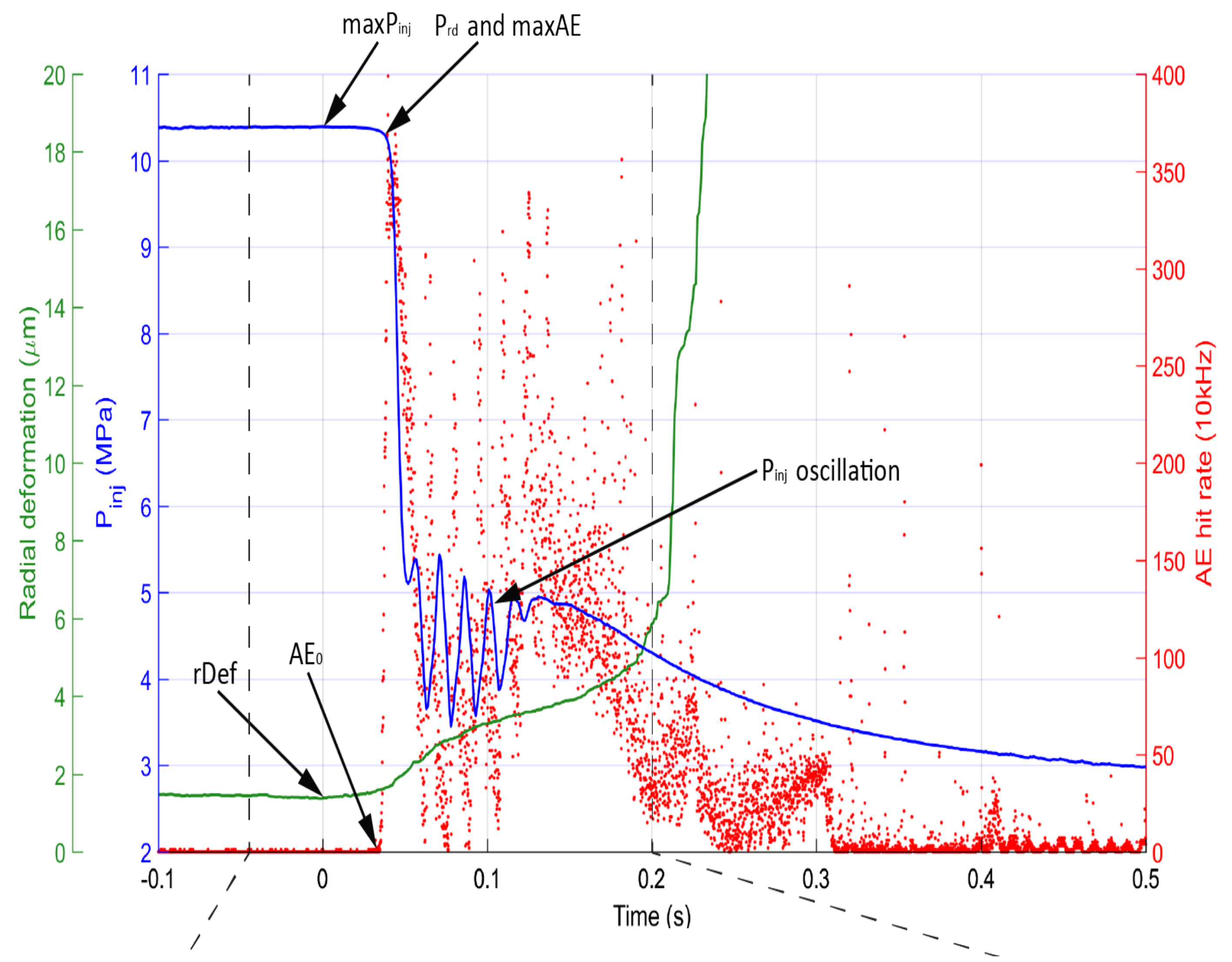

Starting point for analysis: use the AE as a proxy for fracture extension

- Relate cumulative AE energy during each extension of tensile fracture to the proportion of the sample that fracture stage has crossed.
- Equate this to sample geometry, and an initial flaw scale.

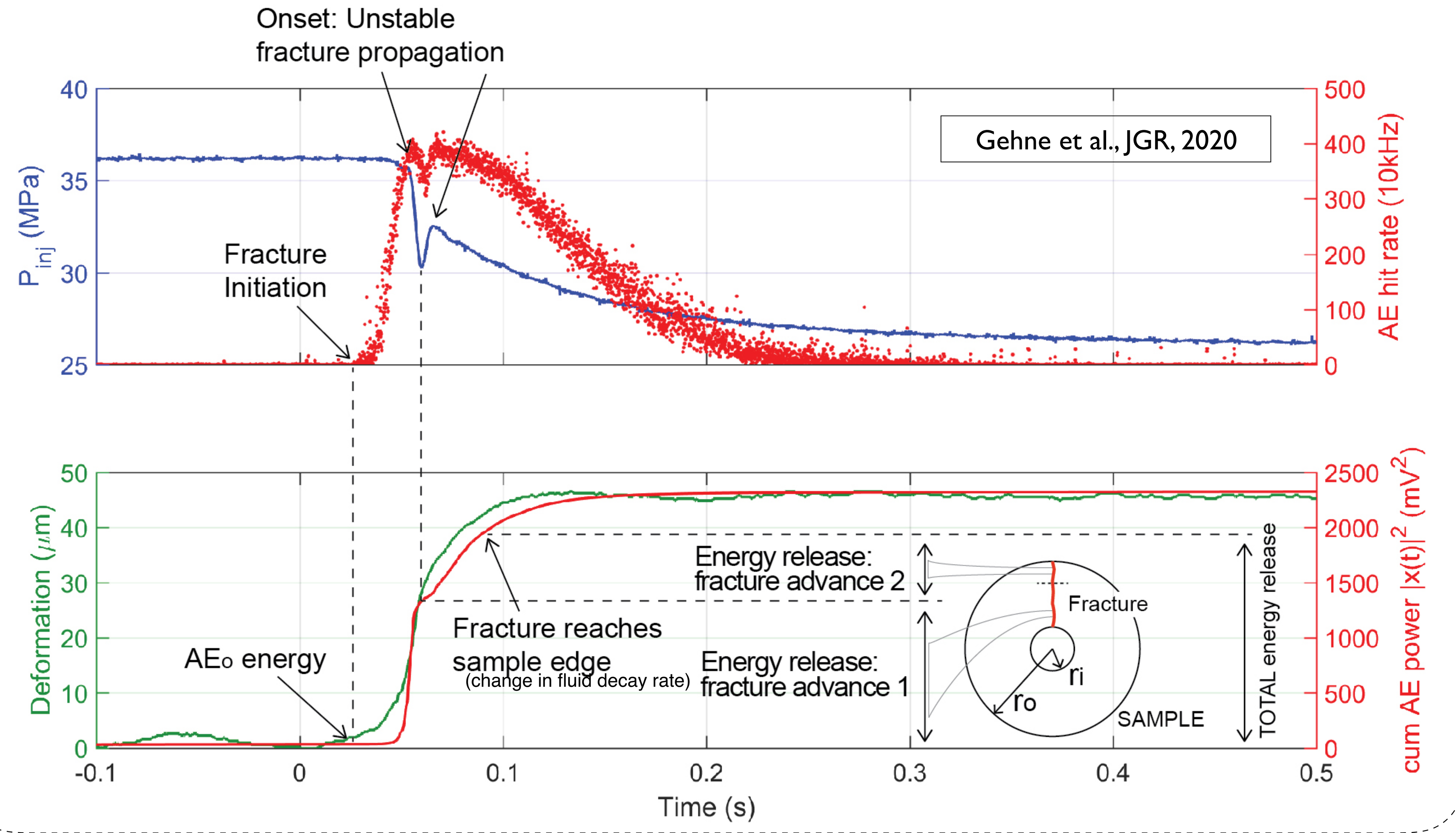

Fluid-driven fracture and seismicity in the shallow crust: Philip Benson, Stephan Gehne, Nathaniel Forbes Inskip, Philip Meredith & Nick Koor

Analysis: using the cumulative energy release as a proxy for cumulative fracture distance extension

To calculate the initial flaw size (before the first fracture event), K_{Ic} as measured using semicircular bend test is applied, via the fracture mechanics model of Abou-Sayed et al. (1978) to estimate (a_0):

$$P_b = P_c + \frac{K_{1c}}{1.2\sqrt{\pi a_0}}$$

Using a two stage example for illustration:

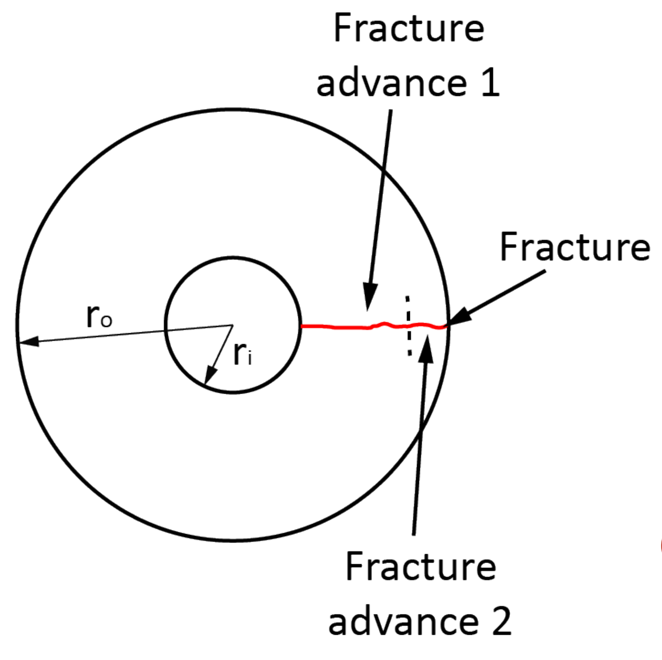

$$\frac{\text{cumulative AE energy at oscillation trough}}{\text{Total cumulative AE energy}} = \frac{\text{flaw length before fracture propagation } (a_0)}{\text{Wall thickness } (r_o - r_i)}$$

OR (for 'n' stages):

$$\boxed{\frac{AE_n}{AE_{tot}} = \frac{a_n}{r_0 - r_i}}$$

Subsequent fracture advances are then calculated iteratively via the cumulative AE ratio to substitute for a_0:

$$eK_{Ic} = \left(P_p - P_c\right)\left[F\left(\frac{a_f}{r_i}\right)\sqrt{\pi a_n}\right]$$

This is essential re-arrangement of the Abou-Sayed equation, where Pp replaces the breakdown pressure Pb on a step by step basis, and with the function F represents the ratio of thick walled cylinder radius to inner radius, taken from Paris & Sih (1965). We denote this an effective K_{Ic} or eK_{Ic}.

Differential pressure

Finally, due to the changing fluid pressure and oscillations, we must also define an 'effective fluid pressure oscillation' at east step:

(12.1 MPa)

$$P_{diff} = P_P - P_c$$

(22 MPa)

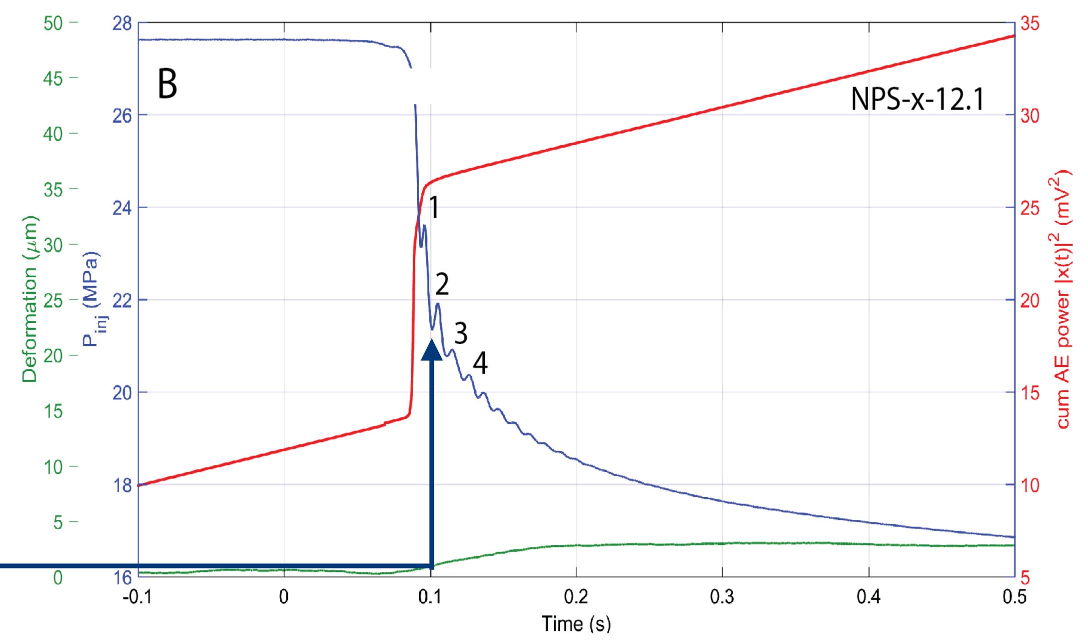

Results: breakdown vs. Confining pressure

8 experiments were chosen for the K_{Ic} analysis from the larger suite of experiments shown earlier, these are shown in the solid symbols:

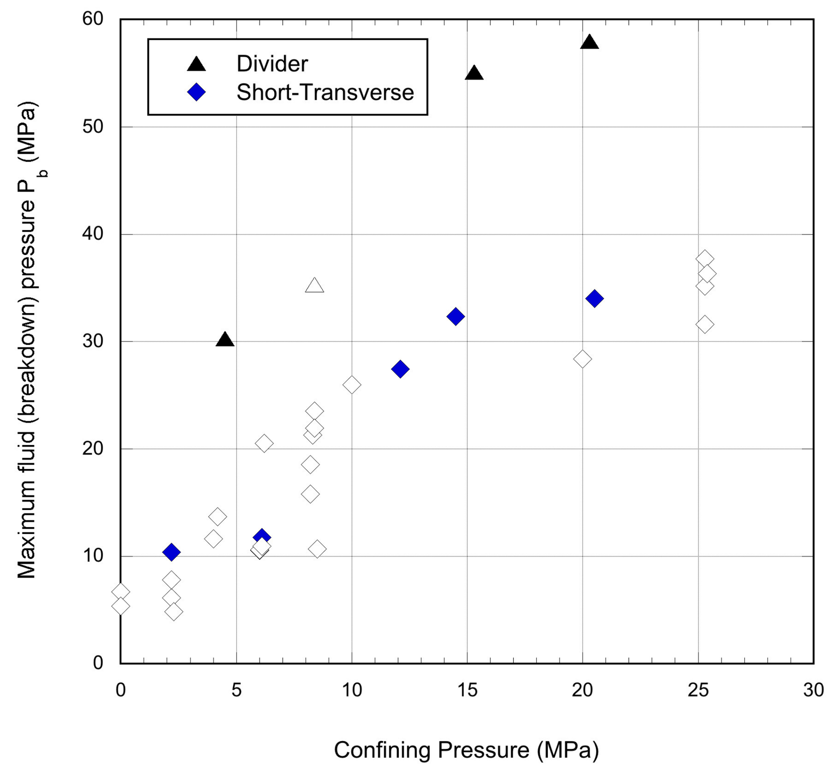

The analysis described is used to determine values of eK_{Ic} for each post-breakdown pressure oscillation in each of the eight experiments (five on ST-orientation samples, and three on divider-orientation samples), across the range of confining pressures applied. Wherever we have a pressure oscillation following initial breakdown, we can calculate the differential pressure required for the associated increment of fracture advance (Pinj - Pc) and the flaw size at the start of that increment of fracture advance.

We recorded a total of 17 pressure oscillations in the eight experiments, and this resulted in a total of 17 calculated values of eK_{Ic} as shown below:

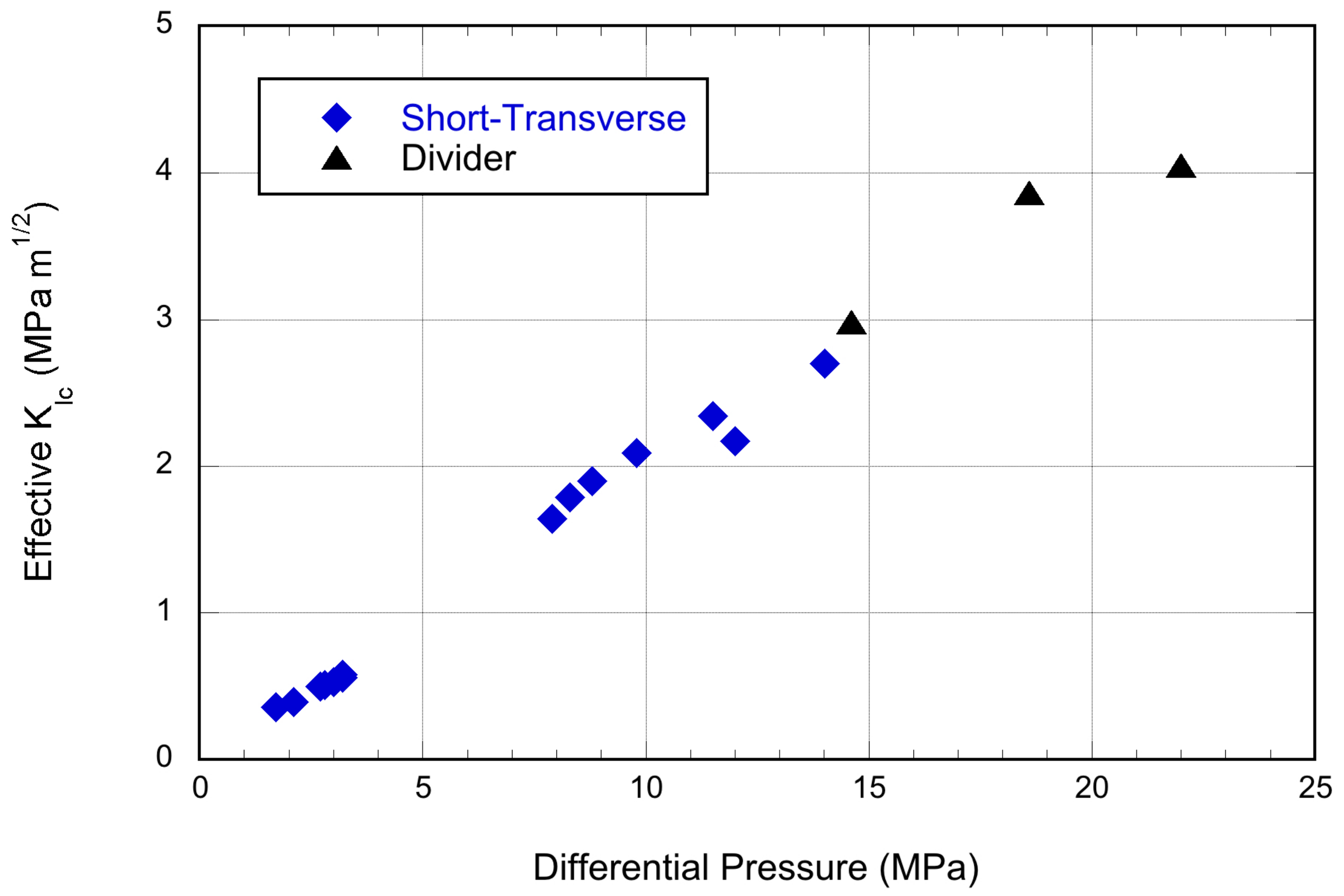

We observe an essentially linear trend, independent of sample orientation, with eK_{Ic} increasing from 0.36 MPa.$m^{1/2}$ to 4.05 MPa.$m^{1/2}$ as the differential pressure increases from 1.7 MPa to 22 MPa.

Discussion points & concluding remarks

We recognize that two key assumptions are involved in determining the effective fracture toughness of Nash Point shale at elevated confining pressure from fluid injection tests on thick-walled cylinder samples:

1. The initial flaw size (a_o), for each fracture orientation, using the ambient pressure values of K_{Ic} from Forbes Inskip *et al.* (2018) and assume that it does not vary with confining pressure.
2. We hypothesize that we can accurately estimate the length of fracture advance for each pressure drop during our fluid injection tests from the proportion of the total AE energy generated during that pressure drop. This then provides the starting flaw size for the following pressure oscillation and fracture advance.

The calculated values of the effective fracture toughness (eK_{Ic}) for each pressure oscillation in all eight of our tests are plotted below as a function of confining pressure:

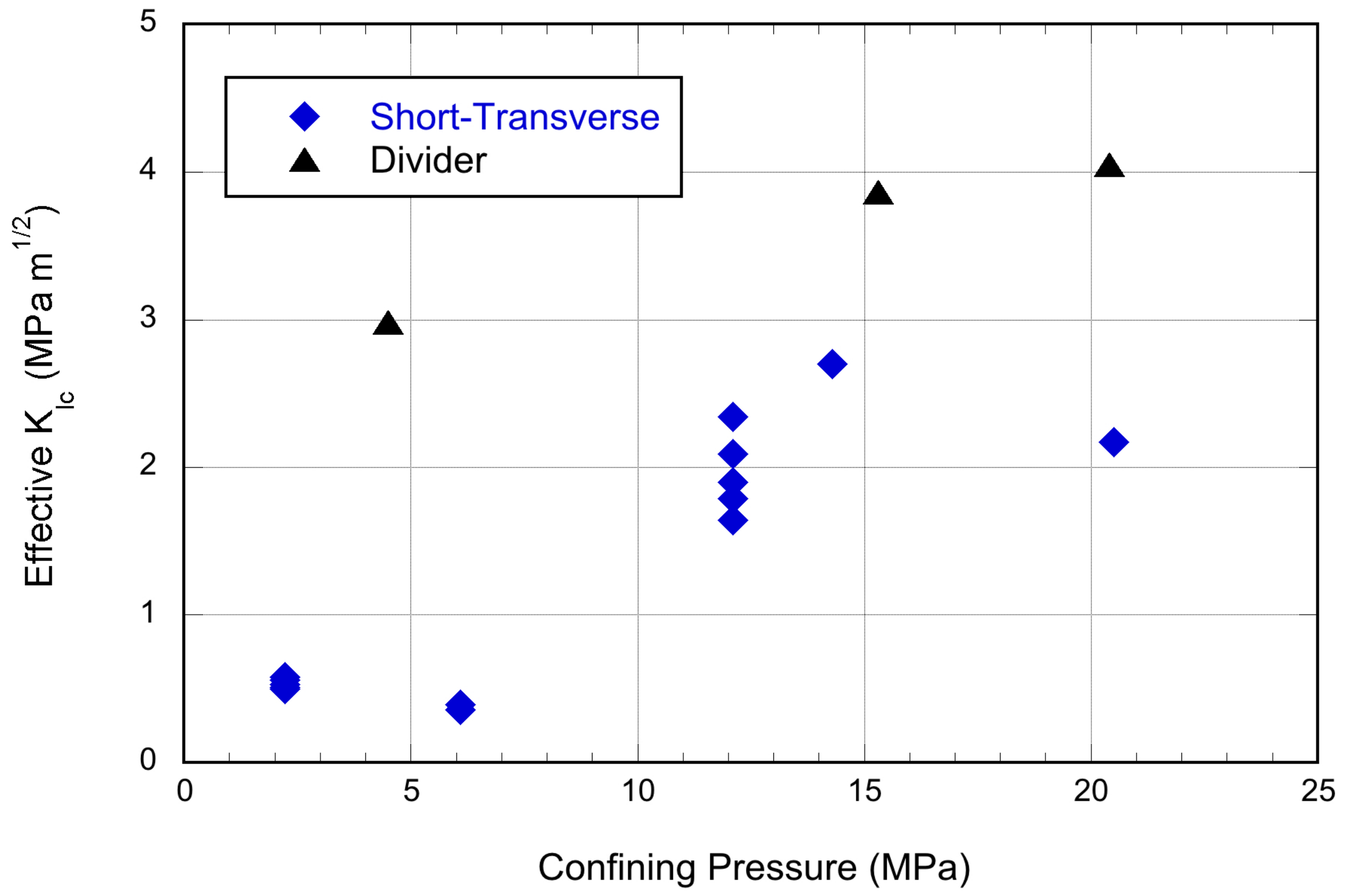

These results confirm that the anisotropy in the fracture toughness of Nash Point shale under ambient pressure conditions previously reported by Forbes Inskip *et al.* (2018) is also maintained at elevated confining pressure. The fracture toughness for the Divider orientation is significantly higher than that for the Short-Transverse orientation for all confining pressures tested. We also observe a general increase in effective fracture toughness with increasing confining pressure in both orientations; with eK_{Ic} increasing to greater than 2 MPa.$m^{1/2}$ in the Short-Transverse orientation and to approximately 4 MPa.$m^{1/2}$ in the Divider orientation at the maximum confining pressure of just over 20 MPa. Extrapolating the Short-Transverse data back to ambient pressure gives a value of 0.22 MPa.$m^{1/2}$, which is very close to the ambient pressure value of 0.24 MPa.$m^{1/2}$ reported by Forbes Inskip *et al.* (2018) for this orientation in Nash Point shale measured using the Semi-Circular Bend methodology (Kuruppu *et al.*, 2014).

We are not aware of any reason why the rate of fracture toughness increase with increasing confining pressure should vary with orientation; nevertheless, extrapolating the Divider orientation data back to ambient pressure gives a value that is significantly higher than the ambient pressure value of 0.71 MPa.$m^{1/2}$ reported by Forbes Inskip *et al.* (2018) for this orientation. If we compare our data with previously published data for other rock types, we find that, when normalized, they fit well within the spread of values summarized in Figure 1.